



## DFT for SnO<sub>2</sub> Doped nanomaterial for Solar Fuel Application

Fatma Zakaria <sup>a</sup>; Sadek, M.A.<sup>a</sup>; Ahmed M.A.<sup>b</sup>; Maryam G Elmahgary <sup>a\*</sup>

<sup>a</sup>Chemical Engineering Department, The British University in Egypt, Cairo, Egypt

<sup>b</sup>Chemistry Department, Faculty of Science, Ain Shams University, Cairo, Egypt



### Abstract

For many years, band gap engineering through defects has been used to develop an efficient photocatalyst. The transparent semiconductor tin oxide (SnO<sub>2</sub>) has been investigated in many research as it has various applications in optical materials due to its transparency, solar cells, biochemical applications, and in catalysis. The electronic along with optical characteristics of co-doping SnO<sub>2</sub> were studied using first principal calculations utilizing the Density functional theory (DFT) with the Generalized Gradient Approximation (GGA) and the Perdew-Burke-Ernzerhof exchange function (PBE). Zinc, Bismuth and Indium have been introduced to the SnO<sub>2</sub> primitive cell as defects in the material with a concentrations  $X_{0.167} Sn_{0.833} O_{2-y} N_y$  where X is (Zn, Bi and In), Y is the concentration of the nitrogen doping which is 0.167. The influence of dopants on the optical and electrical characteristics of SnO<sub>2</sub> was examined in depth after the unit cells were optimized. The study recommends the using of the Bi based tin oxide to be used as a photo catalyst among the investigated structures as it has a band gap near the 1.174 eV and high absorption in the visible light region, low exciton binding energy and smallest D ratio that leads to an enhanced photocatalytic activity compared to the pure SnO<sub>2</sub>.

**Keywords** : SnO<sub>2</sub> ;DFT,Doping electrical properties; optical properties

### 1. Introduction

Global energy depletion, rising environmental pollution, and climatic change are all regarded to be among humanity's greatest issues this century.

The production of solar fuel through photocatalytic water splitting and CO<sub>2</sub> reduction using photocatalysts has attracted considerable attention owing to the global energy shortage and growing environmental problems. [1] SnO<sub>2</sub>, TiO<sub>2</sub>, CeO<sub>2</sub>, and other nano-structured metal (MOs) like have gained interest owing to functional characteristics including high thermal and chemical stabilities, direct bandgap, and optical transparency as well as their present and future uses, including solar cell, transparent conducting electrode (TCE), gas sensor, optoelectronic device, and photovoltaic device. [2-5] Furthermore, it is used as a diluted magnetic semiconductors (DMS) [6].

SnO<sub>2</sub> is an n-type semiconductor with a tetragonal

crystal structure with a large energy of its band gap [7–13]. Doping was also utilized to improve the material's electrical conductivity and transparency in the visible region. [11–12]. As a glaze opacifier [7], polishing powder [8], and protective polymer coating [9] and as a functional material, SnO<sub>2</sub> is primarily used in a variety of applications.

According to theoretical calculations based on fundamental principles, when N is doped to the tin dioxide crystal structure, generates oxygen vacancy, and increases the density of the charges on the tin sites. At the same time, substituting oxygen for nitrogen could reduce CO<sub>2</sub> emissions. Aside from practical studies, there have been numerous theoretical efforts utilizing density functional theory (DFT) to investigate the function of defects like F, S, Sb, and Cl in substitutional locations in SnO<sub>2</sub> [14–22]. They discovered that such doping aids in the development

\*Corresponding author e-mail: [maryam.galal@bue.edu.eg](mailto:maryam.galal@bue.edu.eg)

Receive Date: 16 August 2021, Revise Date: 22 October 2021, Accept Date: 22 January 2022

DOI: 10.21608/EJCHEM.2022.91074.4332

©2022 National Information and Documentation Center (NIDOC)

of single donor states, although the effect of interstitially doped SnO<sub>2</sub> has yet to be investigated.

While there have been some reports of research using cation doping and others investigated anion doping of SnO<sub>2</sub> to improve its performance as a photocatalyst yet, for the best of our knowledge, no one had studied the effect of both anion and cation co-doping of SnO<sub>2</sub> as a potential efficient photocatalyst for hydrogen production via visible light driven water splitting through adjusting both the Conduction Band edge (CB) using suitable cation doping and on the other hand adjusting the Valence Band edge (VB) using suitable anion doping.

Herein, density functional theory (DFT) performing a first principles calculations, has been performed to tune the band gap of SnO<sub>2</sub> and to modify the optical and electrical characteristics of SnO<sub>2</sub>. co-doping SnO<sub>2</sub> with Nitrogen as an anion doping and bismuth, zinc and indium as a cation doping was investigated using Cambridge Serial Total Energy Package (CASTEP) algorithm.

## 2. Methodology

The spin polarized DFT calculations are performed by means of the CASTEP algorithm in this work. The PBE-GGA model was used to express the electron-electron interaction (Perdew-Burke Ernzerhof of the Generalized Gradient Approximation). To account for the interaction between electrons and ions, the Ultrasoft-pseudopotential was used. The Kohn-Sham electrons' wave functions were extended to 400 eV. Regarding the irreducible Brillouin zone, the k points of the Monkhorst-Pack scheme were 5x5x4. The above-mentioned conditions were used to calculate the geometry optimization and generate the density of states profile (DOS). The Hubbard U improvement approach was utilized to appropriately characterize the band gap energies toward overcoming self-interaction inaccuracies in DFT.

In addition, Hubbard U correction was used to get the defect states in the right positions of the edges of the band gap (CB and VB). It also enhances the accuracy of defect formation energies estimations. As a result, the Hubbard U factor utilized was 7 eV and the mean Hellmann-Feynman force value was adjusted to be 0.01 eV/Å. For geometry optimization convergence criterion, whereas the highest displacement tolerance, highest stress permitted, and

energy change allowed are set to  $5.0 \times 10^{-4}$ , 0.02 GPa, and  $5.0 \times 10^{-6}$  eV/atom, respectively.

## 3. Results and discussion

The coordinates of the atoms as well as the lattice constants of SnO<sub>2</sub> was computed and compared to their equivalents in the literature as part of the benchmarking of the structures along with the computational setup. Both theoretical and experimental values were fulfilled by the observed band gap energy and lattice characteristics. With a =4.73 eV, b=4.73 eV, and c=3.19 eV, the band gap energy was 3.61 eV. As a result, the computational setup was authorized for use in the defective structural computations. The 2x2x2 supercell was created to investigate the effects of nitrogen and x doping, where x is (Zn, Bi, and In). Table 1 shows the lattice parameters before and after doping and it is clear that all the dopant atoms of N, Bi and Zn did not make a large distortion to the lattice unit cell (cell volume) which means that there is no additional mechanical stress exerting on the unit cell upon doping. This is mainly ascribed to the small variations between the atomic radii of the initial and doped atoms. The O (48 pm) is replaced by N (56 pm) while Sn (145 pm) is replaced by Bi (143 pm), Zn (142 pm) and In (156 pm). Thus, the only structure that has slightly added stress is the In, N doped structure compared to other structures. The unit cells of the defected structure are as demonstrated in Figures S1-S3.

**Table 1**

Lattice parameters of all the structures

Structure	a (Å)	b (Å)	c(Å)	Vol(Å <sup>3</sup> )	alfa	beta	gamma
SnO <sub>2</sub>	9.47	9.47	6.37	571.261	90	90	90
Zn, N	9.52	9.52	6.37	577.151	90.1	89.8	90.78
Bi, N	9.48	9.48	6.39	574.622	90	90	89.79
In, N	9.56	9.56	6.41	585.436	90	90	90.49

### 3.1. Defect energy

Before deviling into the optoelectronic characteristic, the thermodynamical stability of the defected structure was investigated to address the feasibility of forming the addressed defects as shown in Table 2. Through comparing the energy of the defected structure with the pure energy of SnO<sub>2</sub> which was found to be  $-1.54E^{+4}$  eV using the defect energy

as illustrated in Equation 1. The more negative value of  $\Delta E$  indicates more stable structure than the pure SnO<sub>2</sub> which indicates the thermochemical stability of the formed defects. From this analysis, it is clear that, Indium and zinc co-doped structure are thermodynamically more favorable than the Bi, N structure. However, all the defects are thermodynamically feasible.

Where Defect energy ( $\Delta E$ ) =  $E_{\text{pure SnO}_2} - E_{\text{defected SnO}_2}$

Equation 1 enthalpy change [24]

### 3.2. Electronic Properties

Analyzing the atomic orbitals qualitatively as well as quantitatively are critical in order to gain a thorough analysis of the electronic structure, which has a significant impact on the electronic characteristics of both pure and defected SnO<sub>2</sub>. In order to discover the entity of the defect states as well as investigate the nature of the bonds of all examined defected configurations, the partial density of states (PDOS) was investigated for this endeavor.

#### 3.2.1 PDOS and Band structure

From partial density of states (PDOS) obtained from the DFT calculations, as illustrated in Figures (1-4), it is clear that the calculated pure SnO<sub>2</sub> has a band gap of 3.61 eV which means that it is activated only through the UV part of the sunlight that is accounts only for 4% from the sun light spectrum. The analysis of the PDOS of the pure SnO<sub>2</sub> showed that, its CB of is formed from the Sn 5s orbital while its VB is mainly formed from the O 2p orbital. Thus, in order to engineer the band gap and tune it forward a visible light activity, the selection of the doped atom has to minimize the CB edge and maximize the VB edge to narrow the band gap of SnO<sub>2</sub>. The cation doping of Bi 6s orbital, Zn 3d orbital and In 5s orbital lower the CB as they found to have a CB lower than the CB of Sn 5s while the N 2p orbital doping was found to increase the VB as it has a VB higher than the O 2p orbital.

Regarding the Zn, N structure, it has the minimum band gap energy (1.056 eV) from all the defected structures leading to the highest photo-catalytic efficiency. Bi, N defected SnO<sub>2</sub> structure has a band energy of 1.174 eV which is highly similar to the band gap of Zn, N SnO<sub>2</sub> defected structure. In, N defected SnO<sub>2</sub> structure the highest has a 1.424 eV which is the highest band gap energy from the SnO<sub>2</sub> defected structures. However, it is still much lower than the band gap of the pure SnO<sub>2</sub>. All the defected structures reduce the band gap structure that increases the

efficiency of the defected structures as it will increases the amount of light absorbed and all the defected structure can be used as a photocatalyst from their band gap energy point of view.

The combination of the cation and anion co-doping of N and Bi and Zn creates intermediate delocalized state (shallow state) above the valence band that becomes localized defect states in the case of In, N co-doping. The recombination rates between the electrons and holes are reduced in the case of shallow states thus, Bi, N and Zn, N are more efficient than In, N co-doped photocatalyst for visible light hydrogen production. Moreover, the difference between the oxidation states between the pristine and defected states causes imbalanced atomic charges that would acts as a source of free ions that could facilitate the reaction of water splitting for instance, the difference between the O<sup>2-</sup> and N<sup>3-</sup>.

**Table 2**

Defect energy

Structure	Energy (eV)	$\Delta E$ (eV)
SnO <sub>2</sub>	-1.54E+4	0
Zn, N	-1.68E+4	-0.14
Bi, N	-1.55E+4	-0.01
In, N	-1.67E+4	-0.13

**Table 3**

Effective mass of the electrons and holes

Structure		$mh^*/me$		$me^*/me$	
Pure SnO <sub>2</sub>	Direction	G→F	G→Z	Z→Q	Z→G
	Calculation	0.26	0.12	0.06	0.03
	Average	<b>0.19</b>		<b>0.04</b>	
Zn, N	Direction	G→F	G→Z	G→F	G→Z
	Calculation	0.93	0.80	2.03	2.03
	Average	<b>0.86</b>		<b>2.03</b>	
Bi, N	Direction	G→F	G→Z	G→F	G→Z
	Calculation	3.19	1.73	0.17	0.12
	Average	<b>2.46</b>		<b>0.15</b>	
In, N	Direction	G→F	G→Z	Z→Q	Z→G
	Calculation	2.28	0.44	9.56	4.06
	Average	<b>1.36</b>		<b>6.81</b>	

#### 3.2.2 Effective mass and Exciton binding energy

Both effective mass of electrons and excitons' binding energy are calculated through Equation 2.

$$(1/m^*) = 1/mh^* + 1/me^*$$

Equation 2 effective mass of the electrons [25]

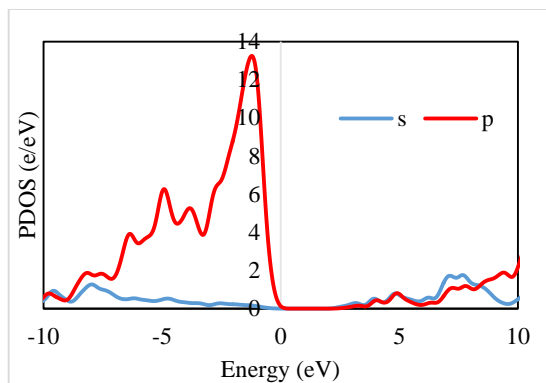
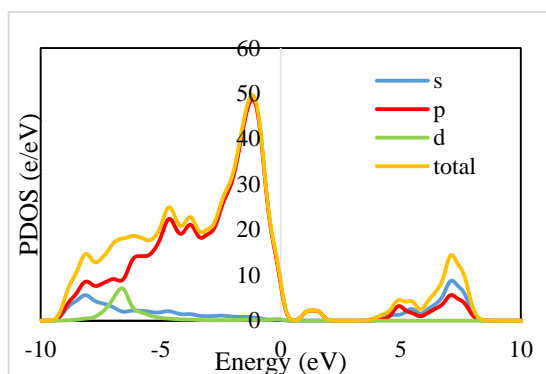
Fig. 1 PDOS of pure SnO<sub>2</sub>

Fig. 2 PDOS of Zn, N

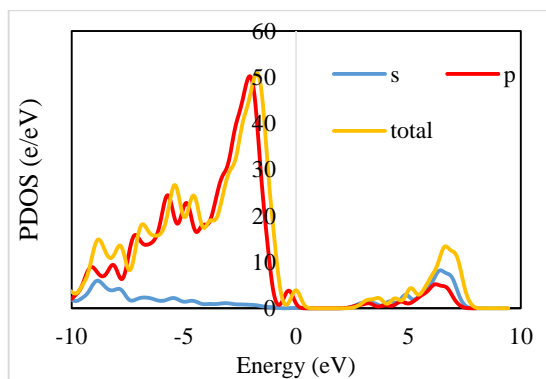


Fig. 3 PDOS of Bi, N

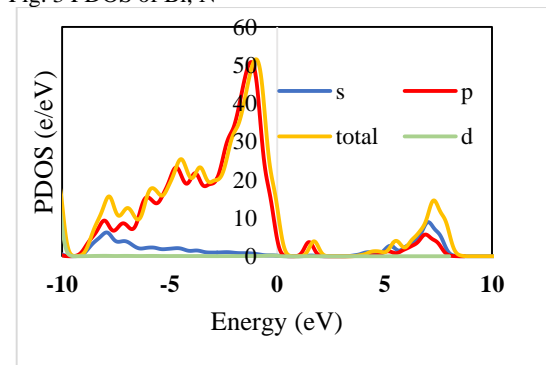


Fig. 4 PDOS of In, N

Where,  $m_{e^*}$  and  $m_{h^*}$  signify respectively, the effective mass of the electrons and the holes,  $m_{\dagger}$  represents the reduced effective masses of the exciton.

The effective mass of the electrons and holes along with the D ratio were calculated as shown in Table 3 and Table 4 using the VB maximum and CB minimum of the band structures points as shown in Figures (S4 - S7).

Regarding the effective mass of electrons and holes, in order to have a high electron mobility which is the first step in the mechanism of water splitting, the mass of the electrons has to be low and the difference between the mass of the electrons and holes has to be high to minimize the recombination rates between the electrons and holes. From the studied defects, Bi, N structure has the lowest mass of electrons which indicates faster response to sunlight and also has the largest mass of holes indicating a minimum recombination rates compared with defected structures and even the pure SnO<sub>2</sub>. Hence, the lowest D ratio (0.06) which is the ratio between the mass of electrons and holes was for the Bi, N co-doped structure. However, the ratio between the holes and electrons are significant in the case of In, N yet, its photo generated electrons are much heavier than all other structures which means it needs more energy to be separate the electrons from the semiconductor that consequently hinders its usage as an efficient photocatalyst.

The photo generated excitons are the first step after the photon absorption, the separated electrons and holes can recombine again but if they have a lower exciton energies they could be separated again. Thus, a lower value of exciton binding energy means easier separation between the holes and electrons refereeing a higher photocatalytic activity. To calculate the exciton binding energy, the reduced mass was calculated using Equation 2. The exciton binding energies ( $R_{ex}$ ) were calculated in Table 5 with the aid of the dielectric constant ( $\epsilon$ ) and the reduced mass as illustrated in Equation 3.

$$E_{ex} \approx 13.56 \frac{m_{\dagger}}{\epsilon r_{me}}$$

Equation 3 Excitons binding energy [26]

The dielectric constant, calculated from figures S9-S11, indicates the optical primitivity of the catalyst and the easiness of the charge carries extraction. It was found that all the co-dopant pairs have approximately the same dielectric constant. However, the Bi, N catalyst shows a slightly higher dielectric constant compared to other doped photocatalyst. On the other hand, the Bi, N co-doped SnO<sub>2</sub> has the lowest value of the exciton binding energies. Thus, in terms of the optical properties and the visible light response, it is

the optimum photocatalyst to be used as an efficient photocatalyst for hydrogen production among other studied catalysts.

**Table 4**

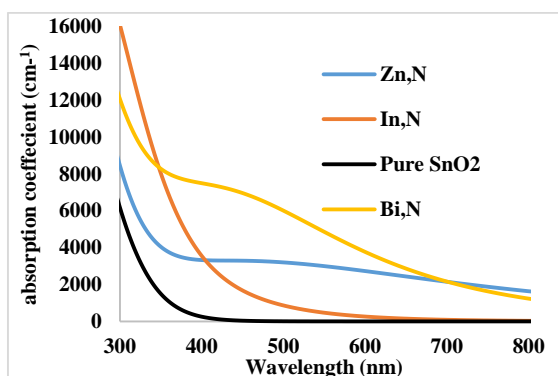
D ratio of the defected structures

Structure	mh*	me*	D
SnO <sub>2</sub>	0.19	0.04	0.25
Zn, N	0.86	2.03	2.35
Bi, N	2.46	0.15	0.06
In, N	1.36	6.81	5

**Table 5**

Exciton binding energy

Structure	$\epsilon_r$	$m^\dagger$	$R_{ex}$ (eV)
Pure SnO <sub>2</sub>	2.24	0.04	0.10
Zn, N	1.914	0.61	2.25
Bi, N	1.976	0.14	0.50
In, N	1.962	1.13	4.01

Fig. 5 absorption coefficient of Co-doped SnO<sub>2</sub>

### 3.2.3 Visible light absorption

For a further analysis to investigate the effects of the co-doping of SnO<sub>2</sub> on the visible light reactivity, the absorption coefficient was calculated using the DFT first principles calculations. The visible light range is approximately from 400 to 700 nm. From the analysis of Figure 9, the pure SnO<sub>2</sub> is activated by sunlight only in the ultraviolet region that ends at 380 nm and it has no activity and completely decay within the visible light region. This outcome is consistent with Figure 1 that illustrates the PDOS of the calculated wide band gap of SnO<sub>2</sub> (3.61 eV) through the high gap between the VB and the CB in Figure 1. The co-doping mechanism followed by this analysis enables a huge rise in the absorption coefficient as shown in Figure 5.

All the studied photocatalyst enhances the efficiency of the SnO<sub>2</sub>, however, the indium doped SnO<sub>2</sub> was the least efficient one as its visible light activity decays after the mid region of the visible light (550 nm). Both zinc and bismuth SnO<sub>2</sub> doped catalyst increases the efficiency of the visible light harvesting

and this finding is compatible with the PDOS of the Zn and Bi as they have a narrow band gaps which enables them to be activated via visible sun light. Thus, they can be used as a visible light photocatalysts. Herein, Bi, N doped SnO<sub>2</sub> is recommended to be used as a photocatalyst for visible light applications to increase the overall photocatalytic process efficiency since the visible light accounts for 43% from the sun light.

## 4. Conclusions

The wide band gap transparent SnO<sub>2</sub> is of great interest due to its applications in optical materials such as, solar cells, biochemical applications, and in catalysis. The main limitation is its wide band gap to efficiently use SnO<sub>2</sub> in the photo-driven applications. To increase its photo activity; both cation and anion doping has been studied. Bi, Zn, and In were used as cation dopants while N as an anion dopant. Despite the Zn, N structure has the minimum band gap energy (1.056 eV) from all the defected structures, Bi, N defected SnO<sub>2</sub> was found to have better electronic properties with band energy of 1.174 eV which is highly similar to the band gap of Zn, N SnO<sub>2</sub> defected structure. In, N defected SnO<sub>2</sub> structure was found to have the highest band gap energy with 1.424 eV. Yet, it is still much lower than the band gap of the pure SnO<sub>2</sub>. On the other hand, the lowest D value is corresponding to the Bi and N defects which means that the effective mass of the electrons is much less than the effective mass of the holes that leads to higher photocatalytic activity. Moreover, Bi, N defected analysis recommends the using of the Bi, N based tin oxide as an enhanced photocatalyst for hydrogen production using the visible sunlight. energy among the other defects that means it has a higher photocatalytic activity and finally it has the lowest D ratio even less than the pure SnO<sub>2</sub>. Hence, among the investigated structures, this detailed analysis recommends the using of the Bi, N based tin oxide as an enhanced photocatalyst for hydrogen production using the visible sunlight.

## Acknowledgments

We would like to express our deep and sincere gratitude to Professor Nageh Allam (The American University in Cairo, School of Science and Engineering, Physics department) for his advice, patience, support, and his fruitful guidance and discussions.

## References

- [1] Mian Zahid Hussain, Zhuxian Yang, Zheng Huang, Quanli Jia, Yanqiu Zhu, Yongde Xia, Recent Advances in Metal–Organic Frameworks Derived Nanocomposites for Photocatalytic

- Applications in Energy and Environment, Advanced Science, 2021, 10.1002/adv.202100625, 8, 14
- [2] Hatem, T., Elmahgary, M.G., Ghannam, R. et al. Boosting dye-sensitized solar cell efficiency using AgVO<sub>3</sub>-doped TiO<sub>2</sub> active layer. *J Mater Sci: Mater Electron*, 2021, 32, 25318–25326.
- [3] C. Rhodes, S. Franzen, J.- Paul Maria, M. Losego, D.N. Leonard, B. Laughlin, G. Duscher, S. Weibel *J. Appl. Phys.*, 2006, 100 Article 054905
- [4] Galal, A.H., Elmahgary, M.G. & Ahmed, M.A. Construction of novel AgIO<sub>4</sub>/ZnO/graphene direct Z-scheme heterojunctions for exceptional photocatalytic hydrogen gas production” *Nanotechnol. Environ. Eng.* ,2021, 6, 5.
- [5] Al-Zaqri, N., Ahmed, M.A., Alsalmeh, A., Galal, A.H., Elmahgary, M.G. “Synthesis of novel direct Z-scheme AgVO<sub>3</sub>-g-C<sub>3</sub>N<sub>4</sub> heterojunction for photocatalytic hydrogen production and bisphenol degradation”. *J Mater Sci: Mater Electron* (2021).
- [6] Ahmet, T. Chikyow, S. Koshihara, H. Koinuma *Science*, 2001, 291, p. 854
- [7] Searle, A.B. *The Glazer’s Book; The Technical Press: London, UK, 1935.*
- [8] Holleman, A.F.; Wiberg, E. *Inorganic Chemistry*; Academic Press: Cambridge, MA, USA, 2001.
- [9] Greenwood, N.N.; Earnshaw, A. *Chemistry of the Elements*; Elsevier: Amsterdam, The Netherlands, 2012.
- [10] Tountas, M.; Topal, Y.; Kus, M.; Ersöz, M.; Fakis, M.; Argitis, P.; Vasilopoulou, M. Water-Soluble Lacunary Polyoxometalates with Excellent Electron Mobilities and Hole Blocking Capabilities for High Efficiency Fluorescent and Phosphorescent Organic Light Emitting Diodes. *Adv. Funct. Mater.* 2016, 26, 2655–2665.
- [11] Batzill, M.; Diebold, U. *The Surface and Materials Science of Tin Oxide. Prog. Surf. Sci.* 2005, 79, 47–154.
- [12]. Fortunato, E.; Ginley, D.; Hosono, H.; Paine, D.C. Transparent conducting oxides for photovoltaics. *MRS Bull.* 2007, 32, 242–247.
- [13] Ching-Prado, E.; Watson, A.; Miranda, H. *J. Mater. Sci.: Mater. Electron.* 2018, 29, 15299–15306.
- [14] Ching-Prado, E.; Samudio, C. A.; Santiago-Aviles, J.; Velumani, S. *J. Mater. Sci.: Mater. Electron.* 2018, 29, 15423–15435.
- [15] Li, W.; Ding, C.; Li, J.; Ren, Q.; Bai, G.; Xu, J. *Appl. Surf. Sci.* 2020, 502, 144140.
- [16] Peng-Fei, L.; Yue, S.; Zhong-Yuan, Y.; Long, Z.; Qiong-Yao, L.; Shi-Jia, L.M.; Li-Hong, H.; Yu-Min, L. Electronic structure and optical properties of antimony-doped SnO<sub>2</sub> from first-principle study. *Commun. Theor. Phys.* 2012, 57, 145.
- [17] Canestraro, C.D.; Roman, L.S.; Persson, C. Polarization dependence of the optical response in SnO<sub>2</sub> and the effects from heavily F doping. *Thin Solid Films* 2009, 517, 6301–6304.
- [18] Rivera, R.; Marcillo, F.; Chamba, W.; Puchaicela, P.; Stashans, A. SnO<sub>2</sub> physical and chemical properties due to the impurity doping. *Lect. Notes Eng. Comp.* 2013, 2, 814–818.
- [19] Velikokhatnyi, O.I.; Kumta, P.N. Ab-initio study of fluorine-doped tin dioxide: A prospective catalyst support for water electrolysis. *Physica B* 2011, 406, 471–477.
- [20] Golovanov, V.; Kuisma, M.; Rantala, T.T. Electron spin resonance parameters of cation vacancies in tin dioxide doped with fluorine and hydrogen. *J. Appl. Phys.* 2013, 114, 143907.
- [21] Oshima, M.; Yoshino, K. Structural and Electronic Structure of SnO<sub>2</sub> by the First-Principle Study. *Mater. Sci. Forum* 2012, 725, 265–268.
- [22] Govaerts, K.; Partoens, B.; Lamoen, D. Extended homologous series of Sn–O layered systems: A first-principles study. *Solid State Comm.* 2016, 243, 36–43.
- [23] Marcillo, F.; Stashans, A. DFT calculations of tin dioxide crystals containing heavily-doped fluorine. *J. Theor. Comput. Chem.* 2014, 13, 1450069.
- [24] Nilsson T and Niedderera, H -Undergraduate students' conceptions of enthalpy, enthalpy change and related concepts, *Chem. Educ. Res. Pract.*, 2014, 15, 336-353
- [25] Kaichen X, Xiaosong L and Ting S, Theory and Ab Initio Calculation of Optically Excited States-Recent Advances in 2D Materials. *Advanced Materials*. 2019, 33, 1904306. 10.1002/adma.201904306.
- [26] Gao, L.-K.; Tang, Y.-L.; Diao, X.-F. First-Principles Study on the Photoelectric Properties of CsGeI<sub>3</sub> under Hydrostatic Pressure. *Appl. Sci.* 2020, 10, 5055.